Factors affecting moment redistribution at ultimate in continuous beams prestressed with external CFRP tendons

Tiejiong Lou, Sergio M.R. Lopes, Adelino V. Lopes

PII: S1359-8368(14)00205-4
DOI: http://dx.doi.org/10.1016/j.compositesb.2014.05.007
Reference: JCOMB 3026

To appear in: *Composites: Part B*

Received Date: 3 February 2014
Revised Date: 9 April 2014
Accepted Date: 9 May 2014

Please cite this article as: Lou, T., Lopes, S.M.R., Lopes, A.V., Factors affecting moment redistribution at ultimate in continuous beams prestressed with external CFRP tendons, *Composites: Part B* (2014), doi: http://dx.doi.org/10.1016/j.compositesb.2014.05.007

Factors affecting moment redistribution at ultimate in continuous beams prestressed with external CFRP tendons

Tiejiong Lou[1], Sergio M. R. Lopes[*1], Adelino V. Lopes[2]

1. CEMUC, Department of Civil Engineering, University of Coimbra, Coimbra 3030-788, Portugal
2. Department of Civil Engineering, University of Coimbra, Coimbra 3030-788, Portugal
(*) – Corresponding author, email: sergio@dec.uc.pt; tel.: +351-239797253

Abstract: A numerical investigation of redistribution of moments in continuous concrete beams prestressed with external carbon fiber reinforced polymer (CFRP) tendons at failure loads is described. A finite element analysis (FEA) model is introduced, and an extensive parametric study is carried out on two-span continuous beams. The factors examined in this study include the content of non-prestressed steel, tendon eccentricities, tendon area, effective prestress, span-to-height ratio, concrete strength, CFRP modulus of elasticity and load type. The results obtained from FEA are compared with those obtained from various codes. The study shows that the importance of some factors is not reflected in the codes. When used to calculate the degree of moment redistribution in these beams, the parameter ε_t (net strain in extreme tension steel) seems to be more reasonable than the parameter *c*/*d* (ratio of neutral axis depth to section effective depth). A simplified equation for calculating the degree of moment redistribution at ultimate is proposed.

Keywords: A. Carbon fiber; B. Strength; C. Finite element analysis (FEA); C. Numerical analysis

1. Introduction

In civil engineering, the use of fiber reinforced polymer (FRP) materials is becoming more and more popular due to their noteworthy advantages of high corrosive resistance and high strength [1]. Extensive efforts have recently been made to examine the overall behavior of FRP-reinforced and strengthened concrete members [2-5]. In the field of external prestressing, FRP composites are promising to be widely used as external tendons for the rehabilitation and construction of various engineering structures. Among the FRP composites, carbon FRP (CFRP) is recognized as an ideal material to replace the conventional prestressing steel. Previous theoretical [6] and experimental [7] studies indicated that external CFRP and steel tendon beams exhibit very similar structural behavior.

In engineering practice, the application of external tendons in continuous concrete beams is rather common. It is well known that the redistribution of moments takes place when a continuous concrete beam begins to assume inelastic behavior. A reasonable consideration of the moment redistribution is important for the flexural strength analysis and design of the continuous beams. Over past years, a number of works have been performed to study the moment redistribution behavior and the factors affecting the redistribution of moments in reinforced [8-11] and bonded prestressed concrete beams [12-14]. However, the studies of the redistribution of moments in continuous concrete beams prestressed with unbounded or external tendons, particularly FRP tendons, are very limited [15,16]. The redistribution of moments is linked to the ductile behavior of concrete beams. Because of the

brittleness of the FRP materials and unbounded nature of external tendons, the concrete beams prestressed with external FRP tendons may exhibit different moment redistribution behavior compared to the conventional concrete beams. As a consequence, the current rules related to the moment redistribution in conventional concrete beams may not be applicable to the external FRP tendon beams.

This paper presents a numerical investigation conducted to evaluate the redistribution of moments in two-span continuous prestressed concrete beams with external CFRP tendons at the ultimate limit state. The results obtained from the finite element analysis (FEA) are compared with those obtained from various codes. A wide range of factors are examined, including the content of non-prestressed tension steel, eccentricities of external tendons at midspan and center support, amount of external tendons, effective prestress, span-to-height ratio, concrete strength, CFRP tendons elastic modulus and type of loading. Based on the results of the parametric analysis, a reasonable simplified equation including the most important parameters for the calculation of the amount of moment redistribution at ultimate is proposed.

2. Measurement of moment redistribution and codes of practice

Several approaches have been used to measure quantitatively the amount of moment redistribution in a statically indeterminate structure. One of the approaches was based on a plastic adaption ratio (PAR) defined by [17]

$$PAR = P_{col} / P_{pl} \tag{1}$$

where P_{col} is the actual ultimate load; and P_{pl} is the ultimate load calculated by a

plastic analysis. $PAR = 1$ indicates full redistribution of moments.

Some investigators [18] defined the plastic adaption ratio using three ultimate loads as follows:

$$PAR1 = (P_{col} - P_{el}) / (P_{pl} - P_{el}) \tag{2}$$

where P_{el} is the ultimate load calculated by an elastic analysis. $PAR1 = 0$ ($P_{col} = P_{el}$) corresponds to zero redistribution, while $PAR1 = 1$ ($P_{col} = P_{pl}$) corresponds to full redistribution.

Cohn [19] defined the degree of moment redistribution by

$$\beta = 1 - M / M_e \tag{3}$$

where M is the actual moment; M_e is the elastic moment calculated based on the theory of elasticity. $\beta = 0$ indicates nil redistribution. This definition is adopted by various codes. In calculating the design moments in continuous flexural members, the codes allow designers to take advantage of a linear analysis with an adjustment of the elastic moments through the use of the degree of moment redistribution β. However, the empirical equations for calculation of β in various codes are quite different.

In the ACI code [20], the degree of moment redistribution for prestressed concrete beams with sufficient bonded reinforcement is calculated using the net strain in extreme tension steel ε_t by

$$\beta(\%) \le 1000\varepsilon_t \tag{4}$$

with a maximum of 20%. Also, the moment redistribution can be done only when ε_t is not less than 0.0075 at the section where the moment is reduced.

The CSA code [21] indicates that the negative moment calculated by an elastic

analysis can be increased or decreased by

$$\beta(\%) \le 30 - 50c/d \tag{5}$$

with a maximum of 20%. In Eq. (5), *c*/*d* is the ratio of the neutral axis depth to the effective depth of a cross section at the ultimate limit state.

In Europe, EC2 [22] and MC10 [23] also uses the parameter *c*/*d* to calculate the degree of moment redistribution:

for $f_c^{'} \le 50$ MPa,

$$\beta \le 0.56 - 1.25(0.6 + 0.0014/\varepsilon_u)c/d \tag{6a}$$

for $f_c^{'} > 50$ MPa,

$$\beta \le 0.46 - 1.25(0.6 + 0.0014/\varepsilon_u)c/d \tag{6b}$$

with a maximum of 30% for high- and normal-ductility steel and of 20% for low-ductility steel. In Eq. (6), $f_c^{'}$ is the concrete cylinder compressive strength; and ε_u is the ultimate concrete compressive strain.

3. Nonlinear model

A previously developed numerical model [24] is used here to conduct the parametric evaluation of the redistribution of moments in continuous concrete beams prestressed with external CFRP tendons. The time-dependent effects are neglected in the present study, but the modeling of these effects can be found elsewhere [25]. The proposed model is based on the finite element method, and accounts for both geometric and material nonlinearities. Apart from the variation in the external tendon depth, the coupling between axial and flexural deformations is also included within

the geometric nonlinearity. The following basic assumptions are adopted in the analysis:

(1) A plane section remains plane after deformations; that is, the strain distribution across the depth of a concrete section is linear.

(2) Non-prestressed steel completely bonds with the surrounding concrete; that is, the strains between bonded reinforcement and concrete are perfectly compatible.

(3) The frictions between deviators and external tendons are negligible. This simplification may lead to a higher predicted stress increase in external tendons at the initial loading stage. After cracking, the tendon stress increases quickly, so the effect of friction loss on the response of load versus tendon stress increase tends to diminish with increasing load up to the ultimate.

(4) The shear deformation is negligible. This simplification is reasonable for slender beams such the ones used for prestressed concrete beams.

The constitutive laws for materials used in the current analysis are as follows:

The stress-strain relationship for concrete in compression suggested by Hognestad [26] is adopted. It is composed of a parabolic ascending branch and a linear descending branch as shown in Fig. 1(a), and is expressed as follows:

for ascending branch,

$$\sigma_c = f_c^{'}\left[\frac{2\varepsilon_c}{\varepsilon_0} - \left(\frac{\varepsilon_c}{\varepsilon_0}\right)^2\right] \tag{7a}$$

for descending branch,

$$\sigma_c = f_c^{'}\left[1 - 0.15\left(\frac{\varepsilon_c - \varepsilon_0}{\varepsilon_u - \varepsilon_0}\right)\right] \tag{7b}$$

where σ_c and ε_c = concrete stress and strain, respectively; f_c' = concrete cylinder compressive strength; ε_0 = 0.002; and ε_u = 0.0038. The concrete in tension is assumed to be linear elastic up to cracking, followed by linear descending stress-strain behavior up to zero stress, as shown in Fig. 1(b) where f_t = concrete tensile strength and ε_{cr} = cracking strain. The CFRP prestressing tendon is linear elastic up to rupture, as shown in Fig. 1(c) where σ_f and ε_f = CFRP tendon stress and strain, respectively; f_f = CFRP tensile strength; and E_f = CFRP modulus of elasticity. The non-prestressed steel is assumed to be elastic-perfectly plastic in both tension and compression, as shown in Fig. 1(d) where σ_s and ε_s = steel stress and strain, respectively; f_y = steel yield strength; and E_y = steel modulus of elasticity.

The concrete beam is divided into a number of beam elements, and the cross section of each element is subdivided into discrete layers to include different material properties. The contribution of external tendons to the concrete beam is made by transforming the current prestressing force into equivalent nodal loads applied on the finite element model. A load control or displacement control incremental method, together with the Newton-Raphson iterative algorithm, is used to solve the nonlinear equilibrium equations of the structure. The iterative procedure for each increment involves four basic steps: (1) form the current tangent stiffness matrix; (2) solve the equilibrium equations; (3) determine the current state for each element; and (4) check convergence. During the solution process, when the concrete strain at the extreme compressive fiber of the critical section reaches the allowed maximum strain, the beam is assumed to be crushed.

The proposed method of analysis is capable of predicting the structural behavior of externally prestressed concrete beams, both simply supported and continuous, over the entire loading range up to the ultimate. The model has been calibrated using a large number of experimental beams available in literature. The comparison between numerical predictions and experimental results for continuous external tendon specimens was reported in Lou et al. [27], where the predicted load-deflection response and stress increase in external tendons were shown to be in favorable agreement with the experimental ones.

4. Parametric study

A two-span continuous prestressed concrete rectangular beam with external CFRP tendons, as shown in Fig. 2(a), is used as a reference beam for the parametric analysis. The material parameters are as follows: unless otherwise stated, the areas of non-prestressed tension steel reinforcement over positive moment region A_{s1} and negative moment region A_{s2} are 720 and 360 mm^2, respectively; the area of non-prestressed compression steel reinforcement A_{s3} is 360 mm^2; the yield strength f_y of non-prestressed steel is taken as 450 MPa; the area of external tendons A_p is 450 mm^2, and the modulus of elasticity E_f and tensile strength f_f of CFRP tendons are 147 GPa and 1840 MPa, respectively; the effective prestress f_{pe} for the CFRP tendons is considered to be 930 MPa; the concrete compressive strength $f_c^{'}$ and tensile strength f_t are 40 and 3 MPa, respectively.

In the finite element idealization, the concrete beam is divided into 36 beam

elements as shown in Fig. 2(b), and the cross section of a beam element is subdivided into 10 concrete layers and two steel layers each of which represents the bottom or top non-prestressed steel reinforcement. The external tendon is also divided into 36 tendon segments corresponding to the beam elements. Using this finite element model, the influence of various factors on the redistribution of moments at ultimate is evaluated. These factors include the non-prestressed steel area, A_{s2}/A_{s1} ratio, tendon eccentricities, tendon area, effective prestress, span-to-height ratio, concrete strength, CFRP elastic modulus and load type. Unless otherwise stated, the results (β, c/d, ε_t) presented in the following sections of this paper are for the critical negative moment (center support) section of the beams at the ultimate limit state.

4.1. Effect of non-prestressed steel area

The effect of non-prestressed steel area is examined by varying A_{s2} from 360 to 2280 mm^2 and maintaining the A_{s2}/A_{s1} ratio at 0.8. Figure 3 shows the variation of β with the amount of non-prestressed steel. Both the FEA results and code predictions are presented. The FEA results are obtained using Eq. (3) where the actual moment capacity M and elastic moment M_e are computed by FEA. In the calculation of M, both geometric and material nonlinearities are considered. On the other hand, in the calculation of M_e, all the materials are assumed to be linear elastic while the geometric nonlinearity is taken into account. In order to obtain the elastic moment M_e, the ultimate load corresponding to the actual moment capacity M is applied and the incremental load method is employed to solve the equilibrium equations. A summary of results in relation to moment redistribution for different amounts of non-prestressed

steel is given in Table 1.

From Fig. 3 and Table 1, it is seen that, according to the FEA predictions, the β value increases with increasing A_{s2} up to 1800 mm^2 and then gradually decreases with continuing increase of the steel area. This observation can be attributed to the combined effects of ductility and stiffness difference between critical sections. When A_{s2} (A_{s2}/A_{s1} = 0.8) increases, the flexural ductility tends to decreases (the less the ductility, the lower the moment redistribution) while the stiffness difference between critical sections enlarges (the larger the stiffness difference, the higher the moment redistribution). Therefore, if the effect of stiffness difference transcends the effect of ductility (for A_{s2} increased up to 1800 mm^2), the moment redistribution increases; on the other hand, if the effect of ductility prevails against the effect of stiffness difference (for A_{s2} increased beyond 1800 mm^2), the moment redistribution decreases.

It is also observed that, according to the predictions by various codes, the moment redistribution consistently decreases as the amount of non-prestressed steel increases. This implies that the codes accounts for the section ductility only, neglecting the stiffness difference between critical sections. As a consequence, the code predictions fail to reflect accurately the actual trend of the variation of β with the amount of non-prestressed steel. In this analysis, it is seen that EC2 and the CSA code are non-conservative particularly at a low amount of non-prestressed steel, while the ACI code is generally conservative.

4.2. Effect of A_{s2}/A_{s1}

The effect of A_{s2}/A_{s1} is examined assuming a minimum non-prestressed steel (A_{s1}

= A_{s2} = 360 mm^2) and varying A_{s1} or A_{s2} from 360 to 1800 mm^2. Figure 4(a) shows the variation of β with the A_{s2}/A_{s1} or A_{s1}/A_{s2} ratio according to FEA predictions. A comparison between the β values predicted by FEA and various code equations is illustrated in Fig. 4(b) and Table 1.

It is observed from Fig. 4(a) that the A_{s2}/A_{s1} (or A_{s1}/A_{s2}) ratio strongly affects the degree of moment redistribution, attributed primarily to the change in the stiffness difference between the critical midspan and center support sections. The β value increases significantly with the increase of A_{s1}/A_{s2} or decreases significantly with the increase of A_{s2}/A_{s1}. When A_{s2}/A_{s1} increases to a level of about 1.6, the positive redistribution at the center support disappears and the negative redistribution begins to appear. The negative redistribution, which indicates that the actual moment is greater than the elastic value, becomes more and more significant with continuing increase of A_{s2}/A_{s1}.

From Fig. 4(b) and Table 1, it is observed that for a fixed value of A_{s2}, the effect of the A_{s2}/A_{s1} ratio is slightly reflected in the ACI code but neglected in other codes where the parameter c/d is used. On the other hand, for a fixed value of A_{s1}, the β values predicted by various codes gradually decreases as A_{s2}/A_{s1} increases, but the importance of the parameter A_{s2}/A_{s1} is significantly underestimated. It should be noted that this observation is attributed to the change in the ductility of the center support section rather than the change in the stiffness difference between critical sections. For a minimum amount of non-prestressed steel over the center support (A_{s2} = 360 mm^2), the ACI code is generally conservative except when the non-prestressed steel over

midspan is close to the minimum amount. The CSA code is non-conservative for A_{s1}/A_{s2} less than about 2, while EC2 is non-conservative for A_{s1}/A_{s2} less than about 3. On the other hand, for a minimum non-prestressed steel over midspan (A_{s1} = 360 mm^2), all the codes are non-conservative, particularly at high values of A_{s2}/A_{s1}.

4.3. Effect of midspan and center support tendon eccentricities

To study the influence of tendon eccentricities on the degree of moment redistribution, four levels of the midspan eccentricity e_1 or center support eccentricity e_2 are selected: 0, 100, 200 and 300 mm. The variation of β with the midspan or center support tendon eccentricity is shown in Fig. 5(a). A comparison between the β values predicted by FEA and various code equations is illustrated in Fig. 5(b) and Table 2.

It is observed from Fig. 5(a) that the β value increases with the increase of e_1 but decreases with increasing e_2. The decreasing rate is much more significant than the increasing rate. The β value increases by 18.5% as e_1 increases from 0 to 300 mm, while decreases by 44.72% as e_2 increases from 0 to 300 mm. The important influence of the tendon eccentricity is partly attributed to the change in the stiffness difference between critical midspan and center support sections, and partly attributed to the change in secondary moments, which is mainly controlled by the profile of the prestressing tendons.

From Table 2, it can be observed that the change in the values of ε_t and c/d with varying e_1 is negligible, indicating that the effect of the variable e_1 is not included in all code equations, as can be seen in Fig. 5(b). On the other hand, as e_2 increases, the value of ε_t remains almost unchanged while the value of c/d quickly decreases. In fact,

the variable e_2 (e_1 as well) does not affect the neutral axis depth c. The significant variation in the value of c/d with e_2 is due to the change of the effective depth, d, of the center support section. From Fig. 5(b) and Table 2, it can also be observed that the effect of the variable e_2 is neglected in the ACI code, while it is incorrectly included in the CSA code and EC2 because the trend predicted by these code equations is opposite to the actual trend by FEA. In addition, the ACI code is conservative while EC2 is non-conservative. The CSA code may be non-conservative for low levels of e_1 or high levels of e_2.

4.4. Effect of tendon area and effective prestress

The tendon area A_p and effective prestress f_{pe} are two variables that determine the effective prestressing force N_{pe} (= $A_p f_{pe}$) that is a fundamental parameter in the design of prestressing. To study the effect of N_{pe} on the moment redistribution, either A_p varies from 0 to 600 mm^2 (f_{pe} = 930 MPa) or f_{pe} varies from 0 to 1240 MPa (A_p = 450 mm^2) so as to produce N_{pe} from 0 to 558 kN.

Figure 6(a) shows the variation of β with the effective prestressing force. It is observed that the β value quickly decreases as the effective prestressing force increases. The phenomenon is particularly obvious when the amount of external tendons varies. When A_p = 0, namely, in the case of a reinforced concrete continuous beam, the β value is as high as 41.55%. The value is significantly reduced to 28.95% when the RC beam is slightly prestressed with external tendons of 150 mm^2. On the other hand, when f_{pe} = 0 (A_p = 450mm^2), the β value is 31.43%, which is much lower than that for A_p = 0.

For different levels of A_p and f_{pe}, a comparison between the β values by FEA and various code equations is illustrated in Fig. 6(b) and Table 3. It is observed in Table 3 that as A_p or f_{pe} increase, the value of ε_t gradually decreases while the value of c/d increases gradually. As a consequence, all the codes take into account the effect of these variables, as shown in Fig. 6(b). It can also be seen that the ACI code is conservative, while EC2 is non-conservative except at a very low level of N_{pe}. The CSA code may be non-conservative at high levels of N_{pe}.

4.5. Effect of span-to-height ratio and concrete strength

Figure 7(a) shows the variation of β with the span-to-height ratio L/h (ratio of span to overall height of a cross section). The results are produced using concrete strengths $f_c^{'}$ of 30 and 50 MPa. For concrete strength of 50 MPa, the maximum redistribution of moments in the beams appears at the ultimate limit state. For concrete strength of 30 MPa, on the other hand, the maximum redistribution of a very slender beam may not take place at ultimate due to softening load-deformation behavior during the loading process. For example, for L/h of 33.33, the maximum redistribution of moments, occurred at the maximum load, is 17% higher than the redistribution at ultimate, as shown in Fig. 7(a). Provided that there is no softening behavior, a higher span-to-height ratio produces an obviously higher redistribution at ultimate, while a lower concrete strength leads to a slightly higher redistribution. However, a long beam with lower concrete strength may exhibit softening load-deformation behavior, hereby causing lower redistribution at ultimate compared to the one with higher concrete strength, as shown in Fig. 7(a).

For different levels of *L*/*h* and $f_c^{'}$, a comparison between the β values by FEA and various code equations is illustrated in Fig. 7(b) and Table 4. It is observed from Table 4 that as *L*/*h* increases, the value of ε_t gradually increases while the decrease in *c*/*d* is negligible, provided that there is no softening load-deformation behavior. Therefore, the effect of *L*/*h* is reflected in the ACI code but neglected in the CSA code and EC2, as shown in Fig. 7(b). It is also observed that a higher concrete strength leads to a higher value of ε_t and a lower value of *c*/*d*, hereby causing higher redistribution according to the code equations. However, this is opposite to the fact that a higher concrete strength produces a lower redistribution as discussed previously. In EC2, the effect of concrete strength is considered using Eq. (6a) for normal-strength concrete and (6b) for high-strength concrete. It is also seen that the ACI code is conservative while EC2 is non-conservative. The CSA code may be non-conservative for a low level of *L*/*h*.

4.6. Effect of CFRP elastic modulus and load type

The CFRP composites cover a wide range of modulus of elasticity which may vary from 80 to 500 GPa [23]. In this study, four levels of the CFRP tendon elastic modulus E_f are selected, namely, 80, 147, 270 and 500 GPa. The corresponding tensile strengths f_f are 1440, 1840, 2160 and 2500 MPa, respectively. Figure 8(a) shows the variation of β with the CFRP modulus of elasticity for center-point loading and uniform loading. It is observed that the β value decreases slightly as E_f increases. In addition, uniform loading mobilizes an obviously higher redistribution compared to center-point loading. In this analysis, the β value for uniform loading is about 1.4

times that for center-point loading.

For different levels of E_f and different types of loading, a comparison between the β values predicted by FEA and various code equations is illustrated in Fig. 8(b) and Table 5. It is observed in Table 5 that the variable E_f affects the values of ε_t and c/d. The load type also influences the value of ε_t but has null effect on the value of c/d. As a consequence, the effect of the variable E_f is considered in all the code equations, while effect of the load type is considered in the ACI code but neglected in the CSA code and EC2, as illustrated in Fig. 8(b). In this analysis, the ACI code is conservative, but may be over-conservative when uniform loading is used. EC2 is non-conservative, particularly for center-point loading. The CSA code may be non-conservative in the case of low CFRP modulus of elasticity and center-point loading.

5. Proposed equation for calculating the degree of redistribution

Among various factors examined in the parametric study, the A_{s2}/A_{s1} ratio is found to be a leading parameter affecting the moment redistribution. The results presented in Section 4.2 (Effect of A_{s2}/A_{s1}) show that the degree of moment redistribution decreases remarkably from 41.97% to -35.35% when A_{s2}/A_{s1} increases from 0.2 to 5 (see Table 1). This indicates that the moment redistribution depends on not only the ductility of one critical section as reflected in the code equations, but also on the structural characteristics of the whole beam. In addition, the parameter ε_t (adopted by the ACI code) seems to be better than the parameter c/d (adopted by the CSA code and EC2) when used to calculate the degree of moment redistribution in continuous

external tendon beams, because ε_t can reflect more important factors affecting the moment redistribution. Therefore, a simplified equation including the two parameters, A_{s2}/A_{s1} and ε_t, may be reasonable to calculate the degree of moment redistribution, since this equation can take into account both the structural characteristics and the section ductility. Based on the above discussion, the ACI code equation indicated by Eq. (4) can be modified as follows:

$$\beta(\%) = \lambda(1000\varepsilon_t) \tag{8}$$

in which λ is a coefficient related to the parameter A_{s2}/A_{s1}. To get the form of λ, the relationship between $\beta/(1000\varepsilon_t)$ and $\ln(A_{s2}/A_{s1})$ for the beams analyzed in Section 4.2 is plotted in Fig. 9. According to the fit curves, λ is related to A_{s2}/A_{s1} by

$$\lambda = 0.65 - 1.2\ln(A_{s2}/A_{s1}) \quad \text{for} \quad A_{s2}/A_{s1} \le 1 \tag{9a}$$

$$\lambda = 0.65 + 0.67\ln(A_{s2}/A_{s1}) - 2.76\ln^2(A_{s2}/A_{s1}) \quad \text{for} \quad A_{s2}/A_{s1} > 1 \tag{9b}$$

Figure 10 illustrates the correlation of simplified equations with the actual β values. In addition to the beams of the present numerical test, 16 two-span unbonded prestressed concrete beam specimens tested by Zhou and Zheng [15] are also used for the correlation. The actual values of β are obtained from FEA (for numerical test specimens) or experiment (for laboratory test specimens). It can be seen from Fig. 10(a) that the data that the ACI code equation is fitted to the actual values are rather scattered. By introducing the coefficient λ, the modified equation proposed in this study correlates well with the actual values, as shown in Fig. 10(b). In addition, most of the data shown in Fig. 10(b) are in the safe side, indicating that the proposed equation is generally conservative in predicting the degree of moment redistribution at

ultimate in such beams.

6. Conclusions

Based on the parametric study conducted on two-span continuous concrete beams prestressed with external CFRP tendons, the following conclusions regarding the redistribution of moments at ultimate can be drawn:

(1) The A_{s2}/A_{s1} ratio is one of the most important factors affecting the moment redistribution. The variation of moment redistribution with the amount of non-prestressed steel depends on the combined effects of ductility and stiffness difference between critical sections.

(2) The redistribution of moments is significantly reduced when a reinforced concrete beam is strengthened by external prestressing. The moment redistribution decreases quickly as the effective prestressing force increases. The eccentricities of external tendons have important influence on the moment redistribution.

(3) A higher span-to-height ratio generally leads to obviously higher moment redistribution. Uniform loading produces much higher moment redistribution than center-point loading. The moment redistribution slightly decreases with the increase of the CFRP tendon modulus of elasticity.

(4) The parameter ε_t (adopted by the ACI code) is superior to the parameter c/d (adopted by the CSA code and EC2) when used to calculate the degree of moment redistribution in continuous external tendon beams, because ε_t can reflect more important factors affecting the moment redistribution.

(5) A simplified equation including two important parameters, A_{s2}/A_{s1} and ε_t, is proposed to calculate the degree of moment redistribution. The proposed equation exhibits a quite good fit to the actual values obtained from FEA and experiment.

Acknowledgments

This research is sponsored by FEDER funds through the program COMPETE – Programa Operacional Factores de Competitividade – and by national funds through FCT – Fundação para a Ciência e a Tecnologia – under the project PEst-C/EME/UI0285/2013. The work presented in this paper has also been supported by FCT under Grant No. SFRH/BPD/66453/2009.

References

[1] Schmidt JW, Bennitz A, Taljsten B, Goltermann P, Pedersen H. Mechanical anchorage of FRP tendons – A literature review. Construction and Building Materials 2012; 32: 110-121.

[2] Seo SY, Feo L, Hui D. Bond strength of near surface-mounted FRP plate for retrofit of concrete structures. Composite Structures 2013; 95: 719-727.

[3] Nigro E, Cefarelli G, Bilotta A, Manfredi G, Cosenza E. Guidelines for flexural resistance of FRP reinforced concrete slabs and beams in fire. Composites Part B: Engineering 2014; 58: 103-112.

[4] Neto P, Alfaiate J, Vinagre J. A three-dimensional analysis of CFRP–concrete bond behavior. Composites Part B: Engineering 2014; 59: 153-165.

[5] D'Antino T, Pellegrino C. Bond between FRP composites and concrete: Assessment of design procedures and analytical models. Composites Part B: Engineering 2014; 60: 440-456.

[6] Lou T, Lopes SMR, Lopes AV. Numerical analysis of behaviour of concrete beams with external FRP tendons. Construction and Building Materials 2012; 35: 970-978.

[7] Bennitz A, Schmidt JW, Nilimaa J, Taljsten B, Goltermann P, Ravn DL. Reinforced concrete T-beams externally prestressed with unbonded carbon fiber-reinforced polymer tendons. ACI Structural Journal 2012; 109(4): 521-530.

[8] Carmo RNF, Lopes SMR. Ductility and linear analysis with moment redistribution in reinforced high-strength concrete beams. Canadian Journal of Civil Engineering 2005; 32(1): 194-203.

[9] Carmo RNF, Lopes SMR. Available plastic rotation in continuous high-strength concrete beams. Canadian Journal of Civil Engineering 2008; 35(10): 1152-1162.

[10] Oehlers DJ, Haskett M, Mohamed Ali MS, Griffith MC. Moment redistribution in reinforced concrete beams. Proceedings of the Institute of Civil Engineers – Structures and Buildings 2010; 163 (SB3): 165-176.

[11] Lou T, Lopes SMR, Lopes AV. Evaluation of moment redistribution in normal-strength and high-strength reinforced concrete beams. ASCE Journal of Structural Engineering 2013; doi: 10.1061/(ASCE)ST.1943-541X.0000994.

[12] Lopes SMR, Harrop J, Gamble AE. Study of moment redistribution in prestressed concrete beams. ASCE Journal of Structural Engineering 1997; 123(5): 561-566.

[13] Kodur VKR, Campbell TI. Evaluation of moment redistribution in a two-span continuous prestressed concrete beam. ACI Structural Journal 1996; 93(6): 721-728.

[14] Kodur VKR, Campbell TI. Factors governing redistribution of moment in continuous prestressed concrete beams. Structural Engineering and Mechanics 1999; 8(2): 119-136.

[15] Zhou W, Zheng WZ. Experimental research on plastic design method and moment redistribution in continuous concrete beams prestressed with unbonded tendons. Magazine of Concrete Research 2010; 62(1): 51-64.

[16] Lou T, Lopes SMR, Lopes AV. External CFRP tendon members: Secondary reactions and moment redistribution. Composites Part B: Engineering 2014; 57: 250-261.

[17] Tichy M, Rakosnik J. Plastic analysis of concrete frames (with particular reference to limit states design). Collet (Publishers) Ltd., London, England; 1977.

[18] Moucessian A, Campbell TI. Prediction of the load capacity of two-span continuous prestressed concrete beams. PCI Journal 1988; 33(2): 130-151.

[19] Cohn MZ. Continuity in prestressed concrete partial prestressing. Partial prestressing, from theory to practice, Vol. I, Survey Reports, NATO ASI Series, Martinus Nijhoff Publishers, Boston, Mass., 1986; 189-256.

[20] ACI Committee 318. Building code requirements for structural concrete (ACI 318-11) and commentary. American Concrete Institute, Farmington Hills, MI; 2011.

[21] CSA. Design of concrete structures. A23.3-04, Canadian Standards Association, Mississauga, Ontario, Canada; 2004.

[22] CEN. Eurocode 2 (EC2): Design of concrete structures – Part 1-1: General rules and rules for buildings. EN 1992-1-1, European Committee for Standardization, Brussels, Belgium; 2004.

[23] FIB. Model Code 2010 (MC10). Bulletins 55 and 56, International Federation for Structural Concrete, Lausanne, Switzerland; 2012.

[24] Lou T, Xiang Y. Finite element modeling of concrete beams prestressed with external tendons. Engineering Structures 2006; 28(14): 1919-1926.

[25] Lou T, Lopes SMR, Lopes AV. Nonlinear and time-dependent analysis of continuous unbonded prestressed concrete beams. Computers & Structures 2013; 119: 166-176.

[26] Hognestad E. A study of combined bending and axial load in reinforced concrete members. Bulletin No. 399, University of Illinois Engineering Experiment Station, Urbana, IL; 1951.

[27] Lou T, Lopes SMR, Lopes AV. Flexural response of continuous concrete beams prestressed with external tendons. ASCE Journal of Bridge Engineering 2013; 18(6): 525-537.

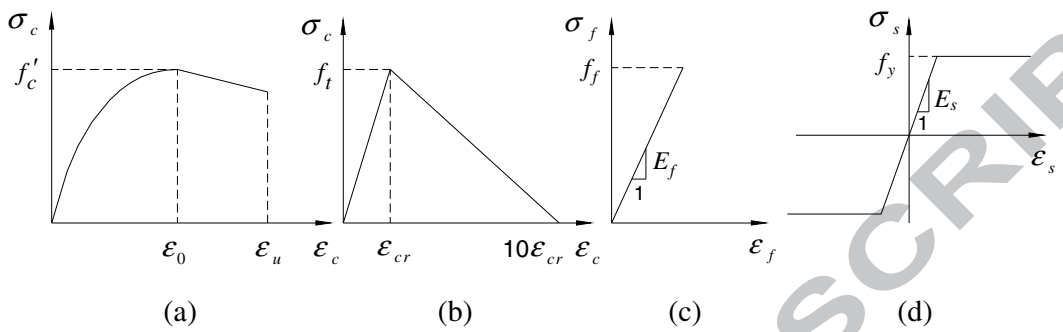

Fig. 1 Stress-strain diagrams for materials. (a) concrete in compression; (b) concrete in tension; (c) CFRP prestressing tendons; (d) non-prestressed steel

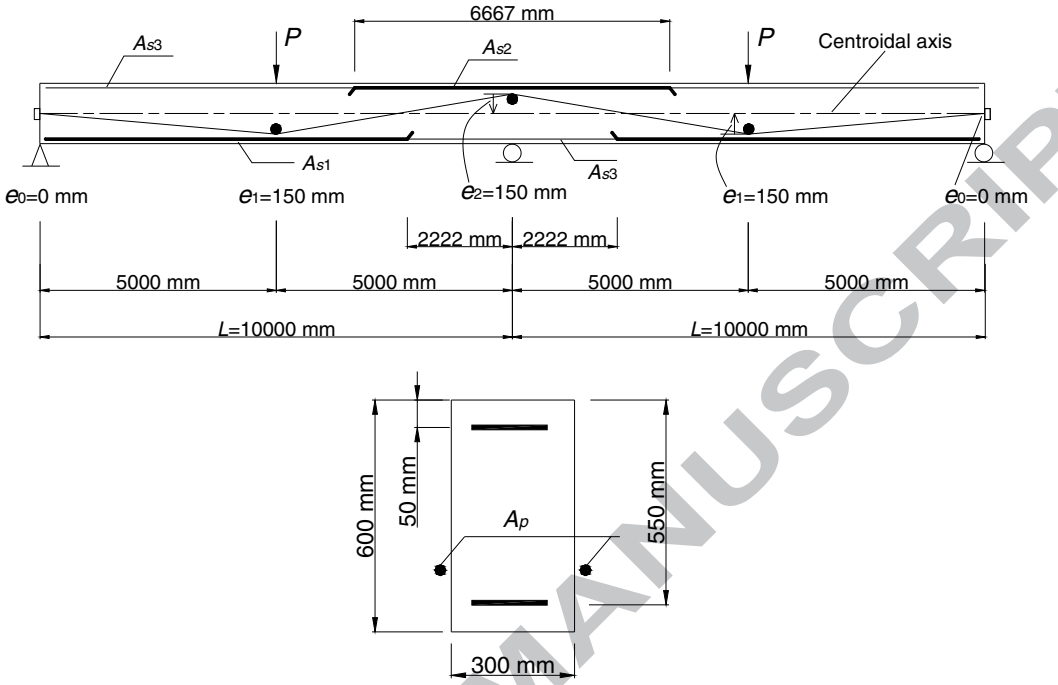

(a)

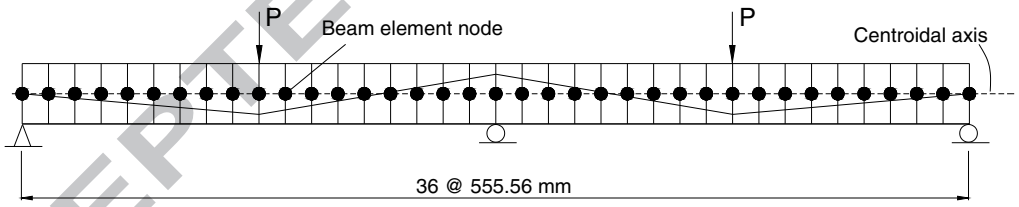

(b)

Fig. 2 Reference beam used for parametric evaluation and its finite element model. (a) beam details; (b) finite element model

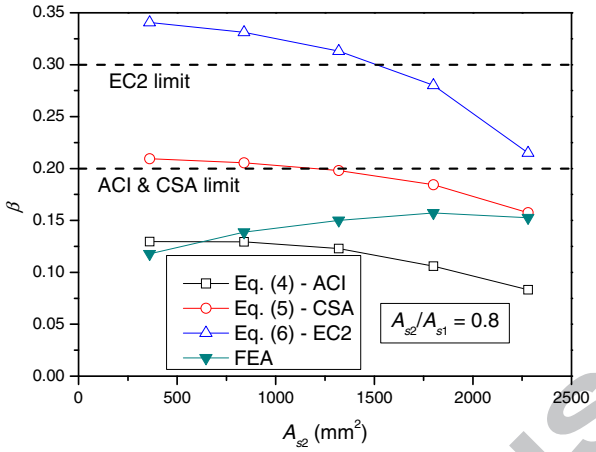

Fig. 3 Effect of non-prestressed steel area on the degree of moment redistribution according to FEA and code predictions

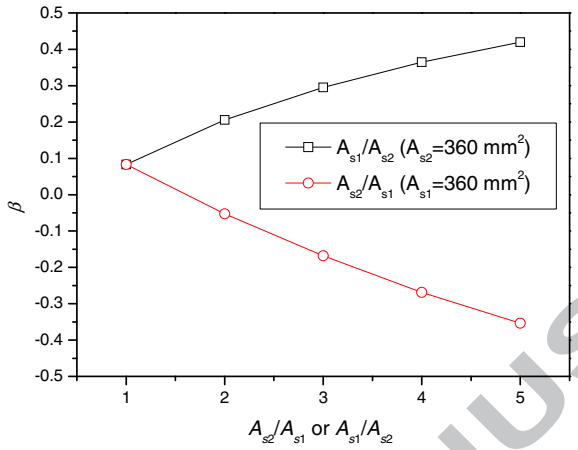

(a)

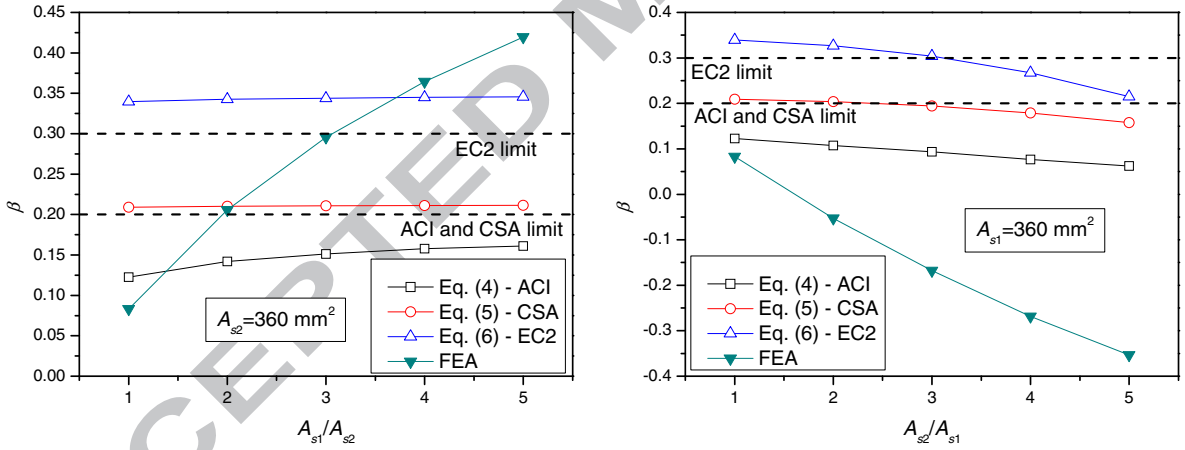

(b)

Fig. 4 Effect of A_{s2}/A_{s1} or A_{s1}/A_{s2} on the degree of moment redistribution. (a) FEA results; (b) comparison between FEA and code predictions

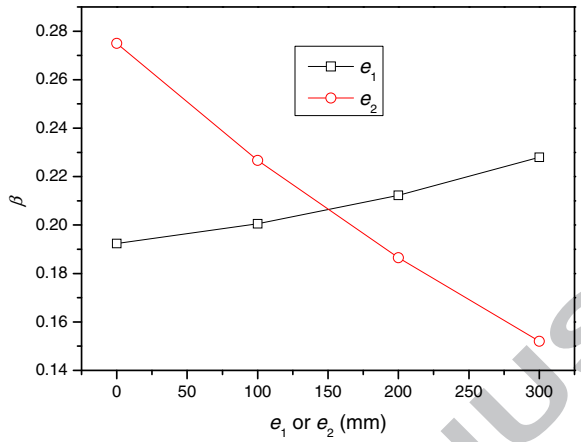

(a)

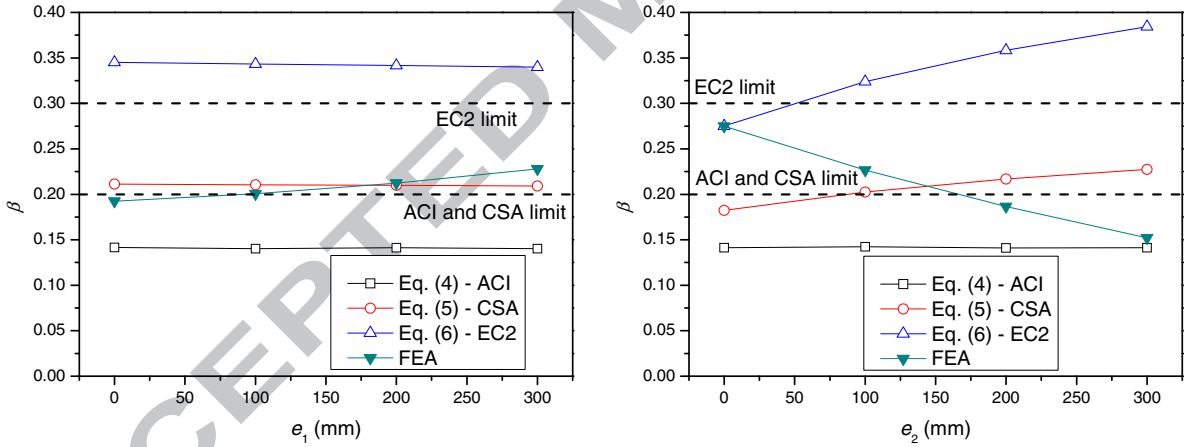

(b)

Fig. 5 Effect of midspan and center support tendon eccentricities on the degree of moment redistribution. (a) FEA results; (b) comparison between FEA and code predictions

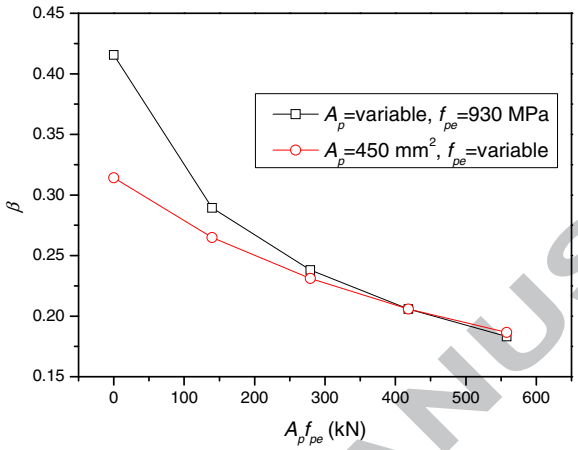

(a)

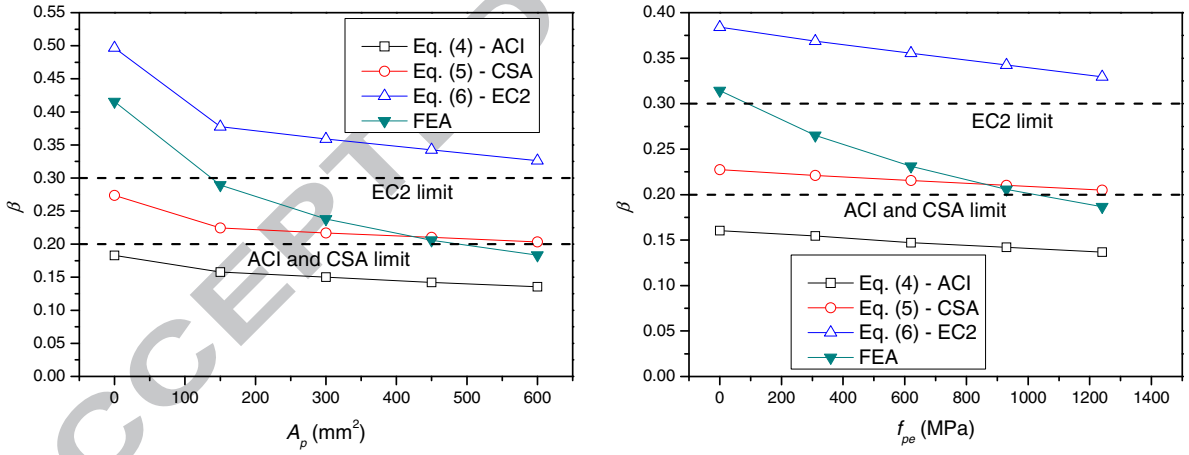

(b)

Fig. 6 Effect of tendon area and effective prestress on the degree of moment redistribution. (a) FEA results; (b) comparison between FEA and code predictions

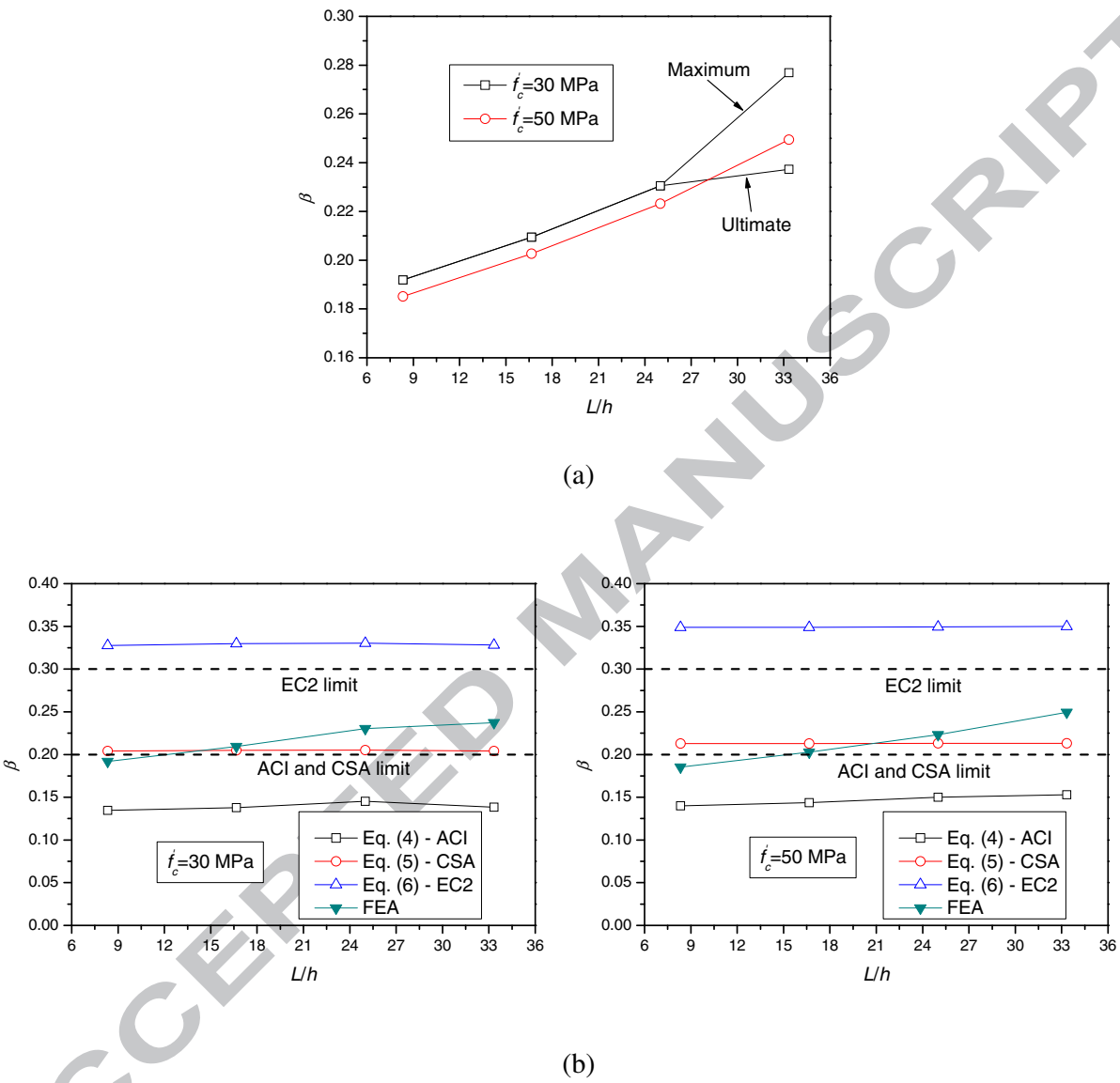

Fig. 7 Effect of span-to-height ratio and concrete strength on the degree of moment redistribution. (a) FEA results; (b) comparison between FEA and code predictions

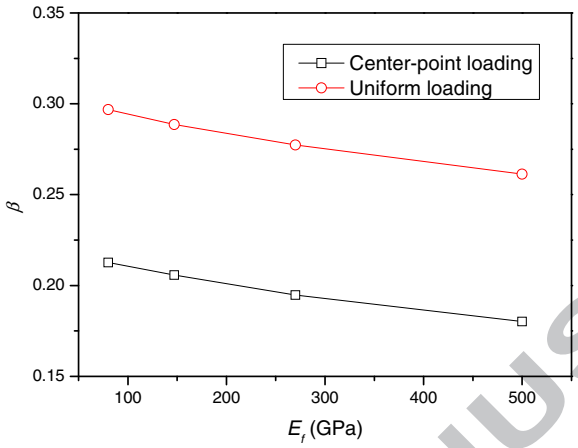

(a)

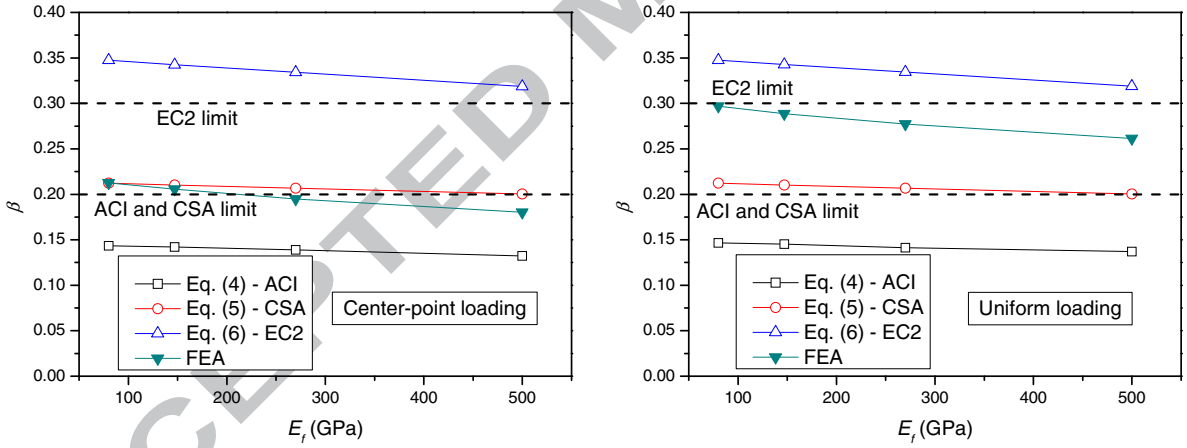

(b)

Fig. 8 Effect of CFRP elastic modulus and load type on the degree of moment redistribution. (a) FEA results; (b) comparison between FEA and code predictions

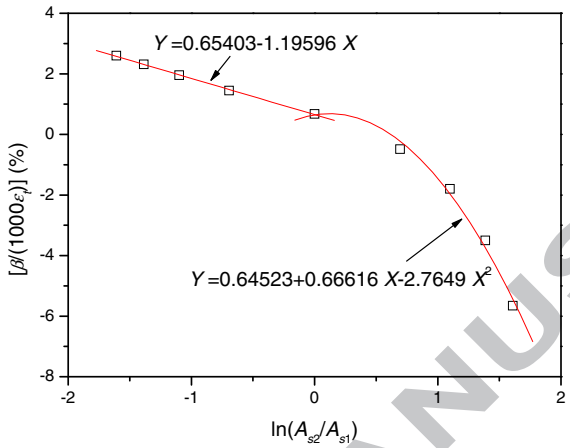

Fig. 9 Relationship between $\beta / (1000\varepsilon_t)$ and $\ln(A_{s2}/A_{s1})$

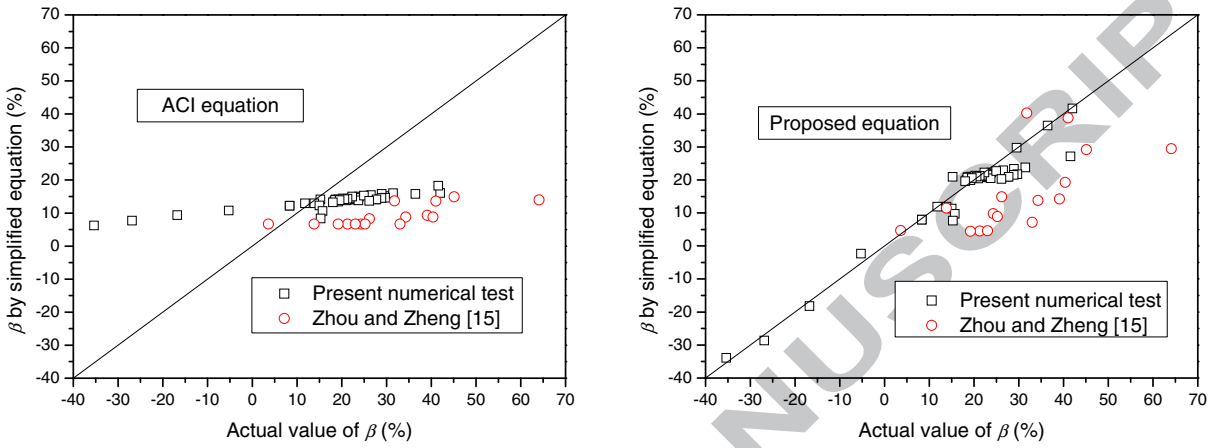

(a) (b)

Fig. 10 Correlation of simplified equations with actual β values. (a) ACI code equation; (b) proposed equation

Table 1 Results in relation to moment redistribution for different contents of non-prestressed steel

Beam	A_{s1} (mm^2)	A_{s2} (mm^2)	A_{s2}/A_{s1}	ε_t (%)	c/d (%)	M (kN·m)	M_e (kN·m)	β (%)			
								Eq. (4) (ACI)	Eq. (5) (CSA)	Eq. (6) (EC2)	FEA
B01	450	360	0.8	1.297	18.11	-327.31	-371.03	12.97	20.94	34.07	11.78
B02	1050	840		1.295	18.90	-444.76	-516.40	12.95	20.55	33.12	13.87
B03	1650	1320		1.230	20.40	-559.45	-658.23	12.30	19.80	31.31	15.01
B04	2250	1800		1.059	23.12	-671.36	-796.61	10.59	18.44	28.02	15.72
B05	2850	2280		0.833	28.50	-781.44	-922.29	8.33	15.75	21.50	15.27
B10	360	360	1	1.226	18.20	-324.37	-353.75	12.26	20.90	33.97	8.31
B11	720		0.5	1.420	17.96	-332.51	-418.69	14.20	21.02	34.26	20.58
B12	1080		0.33	1.512	17.85	-338.38	-480.26	15.12	21.07	34.39	29.54
B13	1440		0.25	1.577	17.77	-342.93	-539.64	15.77	21.12	34.49	36.45
B14	1800		0.2	1.612	17.71	-346.60	-597.30	16.12	21.15	34.56	41.97
B15	360	360	1	1.226	18.20	-324.37	-353.75	12.26	20.90	33.97	8.31
B16		720	2	1.076	19.25	-405.41	-385.15	10.76	20.38	32.70	-5.26
B17		1080	3	0.936	21.13	-486.52	-416.56	9.36	19.44	30.43	-16.79
B18		1440	4	0.768	24.18	-567.80	-447.57	7.68	17.91	26.73	-26.86
B19		1800	5	0.625	28.51	-648.27	-478.97	6.25	15.75	21.49	-35.35

Table 2 Results in relation to moment redistribution for different levels of e_1 and e_2

Beam	e_1 (mm)	e_2 (mm)	ε_t (%)	c/d (%)	M (kN·m)	M_e (kN·m)	β (%)			
							Eq. (4) (ACI)	Eq. (5) (CSA)	Eq. (6) (EC2)	FEA
B21	0	150	1.416	17.75	-320.71	-397.10	14.16	21.13	34.52	19.24
B22	100		1.401	17.91	-328.35	-410.72	14.01	21.05	34.33	20.06
B23	200		1.414	18.03	-336.84	-427.61	14.14	20.99	34.18	21.23
B24	300		1.403	18.18	-344.55	-446.29	14.03	20.91	33.99	22.80
B25	150	0	1.413	23.53	-249.52	-344.16	14.13	18.23	27.52	27.50
B26		100	1.425	19.50	-304.77	-394.10	14.25	20.25	32.40	22.67
B27		200	1.409	16.66	-361.26	-444.11	14.09	21.67	35.84	18.66
B28		300	1.413	14.52	-420.20	-495.53	14.13	22.74	38.42	15.20

Table 3 Results in relation to moment redistribution for different levels of A_p and f_{pe}

Beam	A_p (mm^2)	f_{pe} (MPa)	ε_t (%)	c/d (%)	M (kN·m)	M_e (kN·m)	β (%)			
							Eq. (4) (ACI)	Eq. (5) (CSA)	Eq. (6) (EC2)	FEA
B30	0	930	1.831	5.23	-112.18	-191.93	18.31	27.39	49.67	41.55
B31	150		1.577	15.08	-192.96	-271.56	15.77	22.46	37.74	28.95
B32	300		1.500	16.60	-263.79	-346.26	15.00	21.70	35.91	23.82
B33	450		1.420	17.96	-332.87	-419.12	14.20	21.02	34.26	20.58
B34	600		1.354	19.32	-400.78	-490.69	13.54	20.34	32.61	18.32
B35	450	0	1.605	14.53	-171.98	-250.82	16.05	22.73	38.41	31.43
B36		310	1.545	15.81	-225.48	-306.75	15.45	22.10	36.86	26.50
B37		620	1.471	16.91	-278.69	-362.42	14.71	21.55	35.54	23.10
B38		930	1.420	17.96	-332.87	-419.12	14.20	21.02	34.26	20.58
B39		1240	1.367	19.03	-386.94	-475.71	13.67	20.48	32.96	18.66

Table 4 Results in relation to moment redistribution for different levels of *L*/*h* and $f_c^{'}$

Beam	*L*/*h*	$f_c^{'}$ (MPa)	ε_t (%)	*c*/*d* (%)	*M* (kN·m)	M_e (kN·m)	β (%)			
							Eq. (4) (ACI)	Eq. (5) (CSA)	Eq. (6) (EC2)	FEA
B41	8.33	30	1.346	19.20	-322.16	-398.69	13.46	20.40	32.75	19.19
B42	16.67		1.380	19.01	-324.58	-410.58	13.80	20.49	32.99	20.95
B43	25.00		1.453	18.97	-327.56	-425.66	14.53	20.52	33.04	23.05
B44	33.33		1.383	19.16	-325.00	-426.11	13.83	20.42	32.80	23.73
B45	8.33	50	1.399	17.45	-337.12	-413.73	13.99	21.27	34.87	18.52
B46	16.67		1.438	17.44	-339.61	-425.93	14.38	21.28	34.89	20.27
B47	25.00		1.500	17.39	-342.26	-440.60	15.00	21.30	34.95	22.32
B48	33.33		1.529	17.36	-343.76	-458.01	15.29	21.32	34.99	24.95

Table 5 Results in relation to moment redistribution for different levels of E_f and different types of loading

Beam	E_f (GPa)	Load type	ε_t (%)	c/d (%)	M (kN·m)	M_e (kN·m)	β (%)			
							Eq. (4) (ACI)	Eq. (5) (CSA)	Eq. (6) (EC2)	FEA
B51	80	CPL	1.435	17.56	-312.67	-397.13	14.35	21.22	34.74	21.27
B52	147		1.420	17.96	-332.87	-419.12	14.20	21.02	34.26	20.58
B53	270		1.388	18.65	-368.38	-457.54	13.88	20.67	33.42	19.49
B54	500		1.323	19.93	-428.19	-522.31	13.23	20.03	31.87	18.02
B55	80	UL	1.466	17.54	-330.15	-469.56	14.66	21.23	34.76	29.69
B56	147		1.454	17.94	-352.27	-495.23	14.54	21.03	34.29	28.87
B57	270		1.413	18.63	-389.90	-539.52	14.13	20.68	33.45	27.73
B58	500		1.370	19.93	-455.16	-616.21	13.70	20.04	31.88	26.14

Note: CPL = center-point loading; UL = uniform loading